# *Size Control of FePt Nanoparticles Produced by Seed Mediated Growth Process*

**Hossein Zeynali, Seyed Ali Sebt, Hadi Arabi & Hossein Akbari**

**Journal of Cluster Science**
Including Nanoclusters and Nanoparticles

ISSN 1040-7278
Volume 23
Number 4

J Clust Sci (2012) 23:1107-1117
DOI 10.1007/s10876-012-0506-7


Springer

J Clust Sci (2012) 23:1107–1117
DOI 10.1007/s10876-012-0506-7

ORIGINAL PAPER

# Size Control of FePt Nanoparticles Produced by Seed Mediated Growth Process

**Hossein Zeynali · Seyed Ali Sebt · Hadi Arabi · Hossein Akbari**

Received: 22 May 2012 / Published online: 28 July 2012


**Abstract** Monodisperse FePt nanoparticles with average size of 2.4 nm were successfully synthesized via chemical co-reduction of iron acetylacetonate, $Fe(acac)_3$, and platinum acetylacetonate, $Pt(acac)_2$, by 1,2-hexadecanediol as a reducing agent and oleic acid and oleyl amine as surfactant. Then using the seed mediated growth process smaller sized FePt nanoparticles are used as seeds for the growth of larger sized FePt particles and there is no specific limitation to achieve upper size range by this method. In this work, we could synthesize FePt nanoparticles up to 4.0 nm. Monodispersity with relatively narrow size distribution and having the same elemental composition with the atomic percentage of $Fe_xPt_{100-x}$ ($x = 63$) are the main advantages of this method. As-made FePt nanoparticles have the chemical disordered face centered cubic structure with superparamagnetic behavior at room temperature. After annealing these particles become ferromagnetic with high magnetocrystalline anisotropy and their coercivity increases with increasing particle sizes and reaches a maximum value of 5,200 Oe for size of 46.5 nm

**Keywords** Seed mediated · Co-reduction · FePt · $Fe(acac)_3$ · Monodisperse

## Introduction

FePt magnetic nanoparticles with $L1_0$ phase have been much attention in recent years. These nanoparticles have revealed high uniaxial magnetocrystalline

H. Zeynali (✉) · S. A. Sebt · H. Akbari
Department of Physics, Science and Research Branch, Islamic Azad University,
P.O. Box 14665-678, Tehran, Iran
e-mail: zeynali.ph@gmail.com

H. Arabi
Magnetism and Superconducting Research Laboratory, Physics Department, University of Birjand,
Birjand, Iran

anisotropy. FePt nanoparticles can also be important in many applications, such as: (i) ultra-high magnetic recording media, (ii) high performance permanent magnets, (iii) sensors and drug carriers in biomedical [1]. In order to achieve ultra-high density magnetic recording media, it is limited to the single domain regime so that the system acquires high coercivity. In a high coercivity systems data can be stored for a longer duration. Moreover, small particle sizes (bits) can be approached to enhance areal density. But, the remarkable thing is that these particles (bits) must have high thermal stability. This means that the magnetic anisotropy energy must be larger than thermal energy to minimize thermal fluctuation effects. This will be confine to limitation in nanoparticles size. When the size of particles is less than a minimum critical size, magnetization of the particles becomes unstable and superparamagnetic behavior appears at room temperature, which is unsuitable for magnetic recording media [2]. This minimum critical size for FePt nanoparticles with $L1_0$ phase is about 2.8 nm [3]. Hence, in recent decades great efforts have been made on the chemical methods to achieve a fine controlling on particles size. The chemical solution phase method has been widely applied and is one of the easiest procedures for the synthesis of FePt nanoparticles. In this method, iron and platinum metals salt are used in the presence of surfactant and high boiling point solvents. So far, various iron salt have been considered for the synthesis of FePt nanoparticles. Among of these salts, $Fe(CO)_5$ [4–6], $Fe(OEt)_3$ [7], $Fe(Cl)_2$ [8–11] and $Fe(acac)_3$ [12–16] has been usually used. Types of iron salt, which used in the synthesis process, can play a major and decisive role in controlling the size of nanoparticles. Furthermore, adjusting synthetic parameters such as (i) surfactant, (ii) amount and types of solvent and (iii) heating rate can be considered as the effective parameters in controlling the particle sizes. To obtain FePt nanoparticles with different shapes and sizes by using the $Fe(CO)_5$ precursor, Poydal et al. [17] have changed the ratio of oleyl amine to the oleic acid and also changed the amount of 1,2-hexadecanediol. Simeonidis et al. [18] have found that the types of solvent and heating rate play a crucial role on controlling the size of FePt nanoparticles by using the $Fe(CO)_5$ precursor. Saita and Maenosono [19] are obtained FePt nanoparticles with different sizes by using the $Fe(OEt)_3$ precursor and also by varying synthetic parameters such as, the amount of oleic acid, oleyl amine and the concentration of colloidal solution. Kalogirou et al. [20] also have reported the synthesis of FePt nanoparticles with different sizes by changing the initial molar ratio of $Fe(CO)_5$ to $Pt(acac)_2$. Moreover temperature injection of $Fe(CO)_5$ in the reaction medium is an effective parameter in determining the size of nanoparticles [21, 22]. Changes in the amount of oleic acid and oleyl amine to the $Pt(acac)_2$ precursor is another way to synthesize FePt nanoparticles with different sizes [23]. Liu et al. have shown in their works that the types of iron salt and their physical states have a decisive role in determining the particle size. These results demonstrated that when $Fe(acac)_3$ was used as an iron source, the particles of 2 nm were obtained [24]. In recent years, seed mediated is a conventional method for the producing of magnetic ferrites, $MFe_2O_4$ (M = Fe, Co, Mn,⋯) [25–28]. In this method, synthesized particles in smaller size were used as seeds to produce nanoparticles with larger size. Here, in this work, we could synthesis FePt nanoparticles with sizes larger than 2.4 nm by seed mediated growth process using $Fe(acac)_3$ as the precursors. Monodispersity with relatively narrow

size distribution and controlled growth of the nanoparticles are the advantages of this method. Structural and magnetic properties of the produced nanoparticles were also investigated.

## Experimental

### Synthesis of 2.4 nm FePt Nanoparticle Seeds

$Fe(acac)_3$ (1 mmol), $Pt(acac)_2$ (0.5 mmol), 1,2-hexadecanediol(5 mmol), oleic acid(0.5 mmol), oleyl amine(0.5 mmol) and benzyl ether (20 ml) were mixed together and magnetically stirred under a flow of $N_2$ atmosphere. Mixing was performed for 20 min in order all powder completely dissolved and then heated to 100 °C for 20 min. Reduction of Fe and Pt atoms in the presence of 1,2-hexadecanediol have been obtained and the nucleation of FePt starts to begin. Afterward, the mixture was heated to the boiling point of benzyl ether (300 °C) with heating rate of 5 °C/min in the presence of reflux and kept at this temperature for 15 min before cooling down to room temperature under a flow of $N_2$ atmosphere by removing the heat source. Purification process of the black product was executed as following: 40 ml ethanol was added to the mixture and the black product was precipitated and separated via centrifugation (8000 rpm, 10 min). The ethanol impurities separated and black discarded was dispersed in hexane in the presence of oleic acid (20 μl) and oleyl amine (20 μl). Centrifugation (8000 rpm, 10 min) was achieved again to remove any undispersed residue. Finally, the product 2.4 nm FePt nanoparticles re-disperse in hexane to use for further growth process.

### Synthesis of 3.2 nm via 2.4 nm Seeds

The synthesis of 3.2 nm FePt nanoparticles was achieved by the following: $Fe(acac)_3$ (1 mmol), $Pt(acac)_2$ (0.5 mmol), benzyl ether(20 ml) 1,2-hexadecanediol(5 mmol), oleic acid(0.5 mmol) and oleyl amine(0.5 mmol) in 20 mL benzyl ether at room temperature under a flow of $N_2$ atmosphere. 10 mL hexane solution of as-synthesized 2.4 nm FePt nanoparticles was added as seeds into the reaction medium and the mixture was stirred magnetically for 20 min under a flow of $N_2$ atmosphere, and then was heated to 100 °C for 20 min to remove extra hexane and kept at this temperature for next 20 min. Afterward, the mixture was heated to the boiling point of benzyl ether (300 °C) with heating rate of 5 °C/min in the presence of reflux and kept at this temperature for 15 min before cooling down to room temperature. The black products were centrifuged following the procedure described in the synthesis of 2.4 nm seeds. Finally, 3.2 nm FePt nanoparticles were obtained after a series of centrifugation, which used as seeds to grow larger size particles through seed mediated growth process. Similarly, 10 mL hexane solution of 3.2 nm FePt seeds reacted with $Fe(acac)_3$ (1 mmol), $Pt(acac)_2$ (0.5 mmol), benzyl ether (20 ml) 1,2-hexadecanediol (5 mmol), oleic acid (0.5 mmol) and oleyl amine (0.5 mmol) led to 3.7 nm FePt nanoparticles. Using seed mediated growth process, larger size particles of FePt up to 4.0 nm have been made.

## Nanoparticles Characterization

The structure, morphology, composition and magnetic properties of samples (prepared FePt nanoparticles) were investigated by some equipped analytical systems. Samples for transmission electron microscopy (TEM) analysis were prepared by evaporating the hexane dispersion of particles on amorphous carbon coated copper grids. The TEM images were recorded using a LEO system, model 9120 AB, working at 120 kV. The HRTEM image were recorded using a JEM-2100 model working at 200 kV. ImageJ software has been used to calculate the histogram and average size of FePt nanoparticles. For calculation the average size of FePt nanoparticles, using this software, all the particles in TEM images have been considered. Energy-dispersive X-ray spectroscopy, EDS (15 kV), was performed to determine the elemental composition of FePt nanoparticles. X-ray powder diffraction, STOE diffractometer with Cu-K$\alpha$ source ($\lambda = 1.5405$ Å), was used for studying the crystallinity of FePt nanoparticles and finally magnetic measurements were carried out using a vibrating sample magnetometer (Lake Shore 7410) with the maximum field up to 20 kOe.

## Results and Discussion

Figure 1 shows the X-ray diffraction patterns (XRD) of as-synthesized FePt nanoparticles with different sizes (from 2.4 to 4.0 nm). It can be seen that the full width of half maximum of (111) peak at $2\theta = 40.4°$ decreases as the particles size

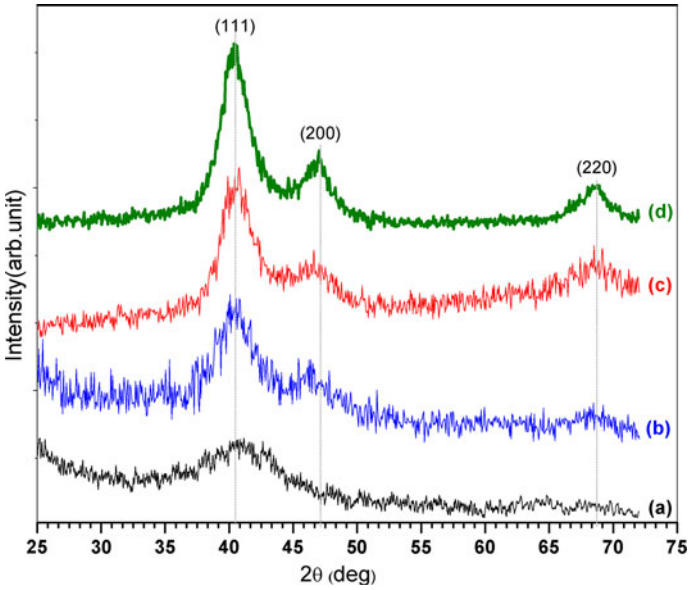


**Fig. 1** XRD patterns of as-synthesized FePt nanoparticles with the average size of (**a**) 2.4 nm (**b**) 3.2 nm (**c**) 3.7 nm (**d**) 4.0 nm

increase due to growth of larger crystallites. With reducing the FWHM of (111) peak, two peaks assigned to (200) and (220) appear at $2\theta = 47.1$ and 68.6°, respectively. With increasing the size of nanoparticles, these peaks become clear in Fig. 1d, which are attributed to the face centered cubic (fcc) structure.

TEM analysis that as-synthesized FePt nanoparticles in the first step and prepared by seed mediated growth process are nearly monodisperse. Figure 2a shows the TEM image of as-synthesized FePt nanoparticles (average size of 2.4 nm) which have spherical shapes and well isolated. Figure 2b–d shows the TEM image of FePt nanoparticles with different sizes (average size of 3.2, 3.7 and 4.0 nm respectively). It is observed that seed mediated growth process can be an appropriate method for increasing the size of nanoparticles and also yields to nearly monodisperse FePt nanoparticles, which the assembled nanoparticles are individually isolated and uniformly distributed. To illustrate single crystal of FePt, an enlarged HRTEM image and electron diffraction pattern were prepared. The HRTEM image of 4.0 nm FePt nanoparticles and electron diffraction pattern shows that each particle is single crystalline and reveals good crystallinity and clear lattice fringes as shown in Fig. 2e, f, respectively.

Figure 3a–d is the histogram of FePt nanoparticles with different sizes. The standard deviation ($\sigma$) of FePt particles are about 0.6, 0.5, 0.7 and 0.9 nm for particles with average size of 2.4, 3.2, 3.7 and 4.0 nm, indicating relatively narrow size distributions ($\sigma/<d>$) equal with 0.25, 0.15, 0.18 and 0.22 respectively.

The formation of the nanoparticles is performed in two steps: nucleation and growth. In the nucleation step, by heating the reaction medium to a high temperature, the precursors chemically transform into the reactive atomic or molecular spices (monomers). In this situation, supersaturation of monomers occurs and nucleation an initial seed is formed. The nuclei then grow due to incorporation additional monomer still present in the reaction medium. There is a critical size at any given concentration of monomers. According to the size-distribution focusing nanocrystal growth curve [29], the formed particles, which their size are smaller than the critical size, were unstable and have a negative growth rate, which means that particles are dissolved and larger particles that have a positive growth rate will grow. The growth process is extremely dependent on the concentration of monomers. At a high monomer concentration, the critical size is small so that all the particles grow and at low monomer concentration, critical size has increased, as a result smaller particle dissolved and larger ones grow [30]. In the present work and via the chemical polyol method and using the seed mediated growth process FePt nanoparticles with sizes larger than 2.4 nm were synthesized. In this process synthesized particles, which their growth are complete simultaneously with new precursors injected into the reaction medium and then heated. By heating precursors transformed into the reactive atomic or molecular spices (monomers). Nevertheless, due to the presence of formed particles (synthesized seeds at first step) in the reaction medium, most of the monomers do not participate in nucleation. Therefore, monomer concentration increases and particles grow due to incorporation of additional monomer into the reaction medium. In this situation, smaller particles grow faster than the larger ones and as results the size distribution can be narrowed.

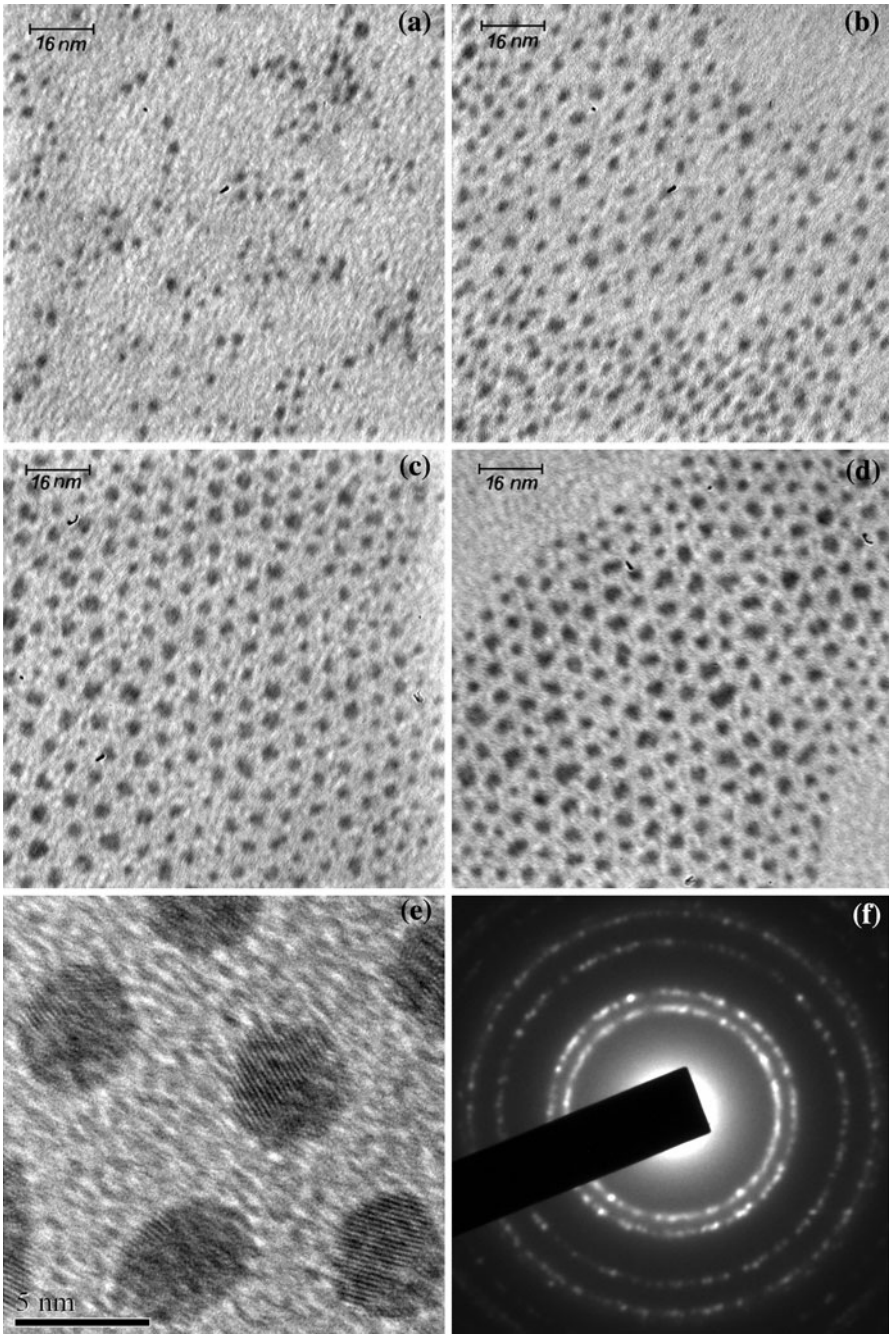


**Fig. 2** TEM images of as-synthesized FePt nanoparticles with the average size of (**a**) 2.4 nm (**b**) 3.2 nm (**c**) 3.7 nm (**d**) 4.0 nm and (**e**) HRTEM images, (**f**) electron diffraction pattern of as-synthesized 4.0 nm FePt nanoparticles

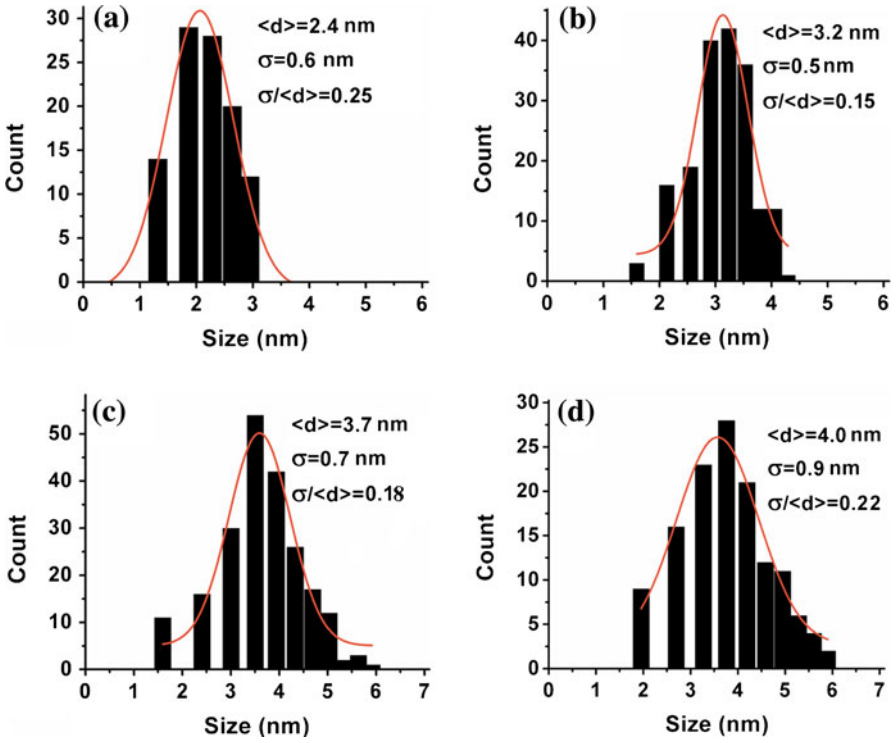


**Fig. 3** Histogram analyses of as-synthesized FePt nanoparticles with the average size of (**a**) 2.4 nm (**b**) 3.2 nm (**c**) 3.7 nm (**d**) 4.0 nm

Figure 4 shows the elemental composition analysis of FePt nanoparticles with different sizes. Average atomic percentage of nanoparticles is about $Fe_{63}Pt_{37}$, suggesting that the seed mediated growth process did not any effect on their FePt phase structures, only the size of nanoparticles has been changed. So the elemental composition ratio regards to the particle sizes, respectively equal $\frac{63.16}{36.84}$, $\frac{62.36}{37.64}$, $\frac{63.47}{36.53}$ and $\frac{64.72}{35.28}$.

Since, as-synthesized FePt nanoparticles have fcc structure with A1 disordered phase, annealing at high temperature (700 °C for 1 h) in forming gas (93 % Ar + 7 % $H_2$) is required to phase transformation from fcc structure to fct structure. As shown in the Fig. 5, in each diffraction patterns, the (111) peak of annealed FePt nanoparticles shifted to 41.4° and super lattice (110) and (001) peaks showed up after the annealing, indicating the formation of the $L1_0$ ordered phase with fct structure. Other peaks that attributed to the fct-$L1_0$ structure are: (200) (002) (220) and (202). By the annealing process, organic surfactant (oleic acid and oleyl amine) start to decompose at a temperature above 350 °C and due to that sintering of particles take place and particles size become larger than before. Average diameters of annealed particles were calculated from the peak broadness of the (111) by using Scherrer equation [31] and their size are about 16.7, 34.3, 41.4 and 46.5 nm in the Fig. 5a–d, respectively.

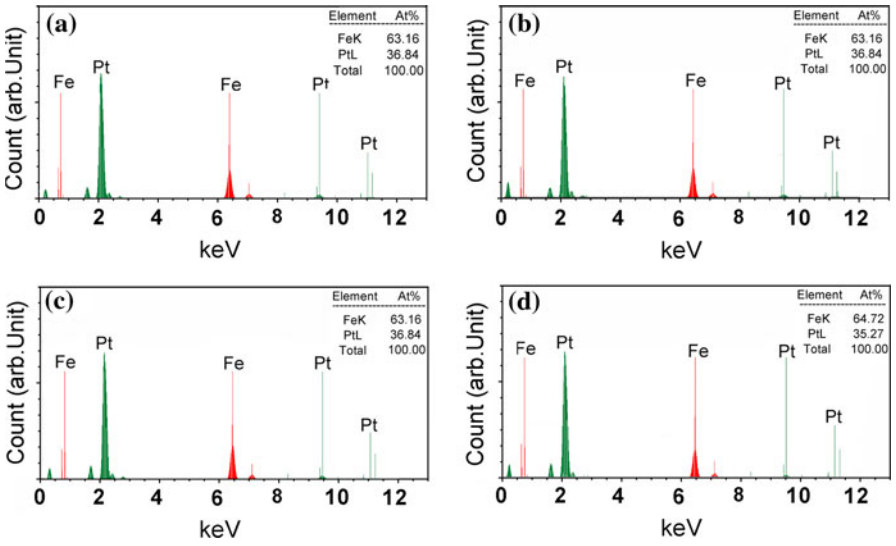


**Fig. 4** EDS spectrum of as-synthesized FePt nanoparticles with the average size of (**a**) 2.4 nm (**b**) 3.2 nm (**c**) 3.7 nm (**d**) 4.0 nm

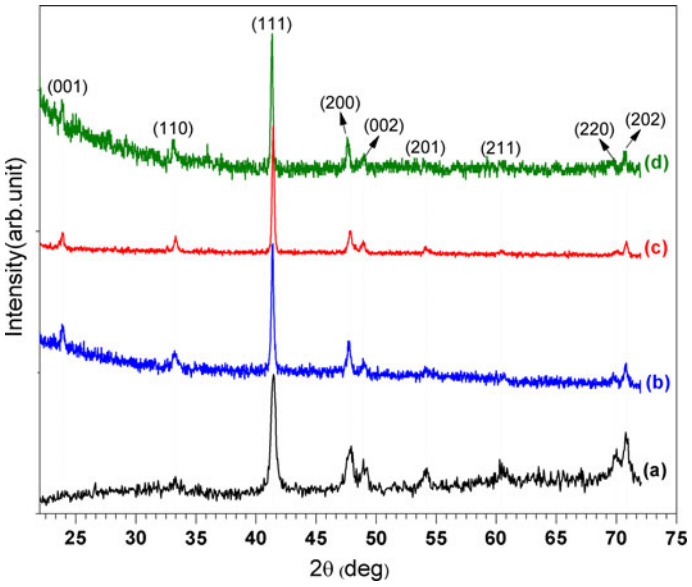


**Fig. 5** XRD Patterns of annealed FePt nanoparticles at 700 °C with the average size of (**a**) 16.7 nm (**b**) 34.3 nm (**c**) 41.4 nm (**d**) 46.5 nm

Figure 6 shows the hysteresis loops of as-synthesized FePt particles with different sizes. The as-synthesized FePt nanoparticles have chemically disordered fcc structure and are superparamagnetic at room temperature due to their low magnetic anisotropy. This means that the thermal energy at this temperature can

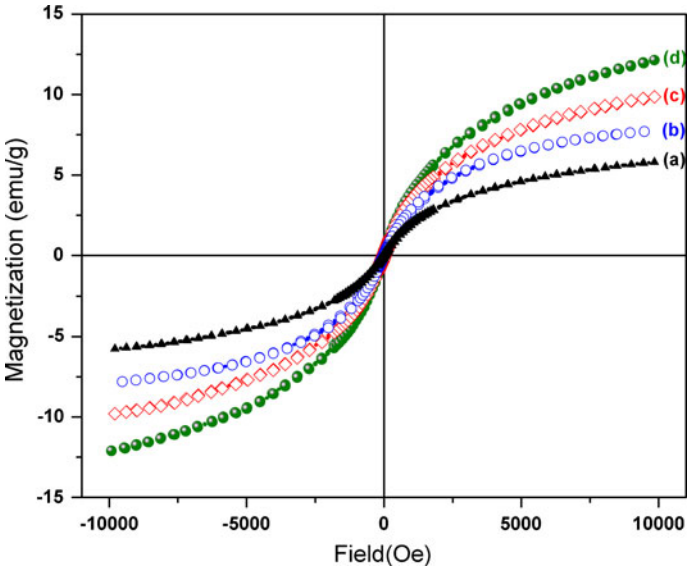


**Fig. 6** Hysteresis loops of as-synthesized FePt nanoparticles with the average size of (**a**) 2.4 nm (**b**) 3.2 nm (**c**) 3.7 nm (**d**) 4.0 nm

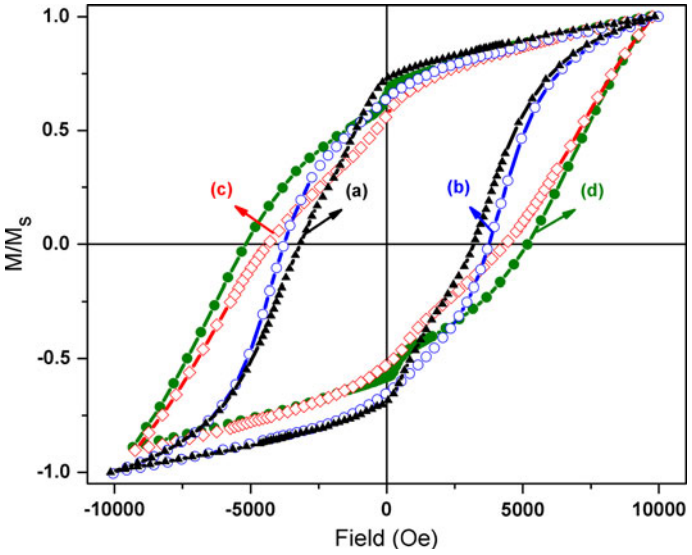


**Fig. 7** Hysteresis loops of annealed FePt nanoparticles at 700 °C with the average size of (**a**) 16.7 nm (**b**) 34.3 nm (**c**) 41.4 nm (**d**) 46.5 nm

overcome the anisotropy energy barrier of the single particles, and the magnetization vectors of these nanoparticles are oriented in the opposite directions (randomly), so the net magnetization of the nanoparticles assemblies is zero in the absence of an external field.

Figure 7 shows the hysteresis loops of annealed FePt particles. As shown in Fig. 7, coercivity increases with increase the particle sizes and reaches a maximum value of 5,200 Oe for average size of 46.5 nm. Appearing high coercivity after annealing similar the results of XRD, indicating the formation of $L1_0$ ordered phase at 700 °C for 1 h. Such magnetic behavior can be explained with coherent rotation model (Stoner–Wohlfarth Model) for single domain magnetic particles.

## Summary

Since, the various synthesis parameters unable to make significant changes in the size of the FePt nanoparticles which are produced by $Fe(acac)_3$ precursor. In this work, seed mediated growth process has been proposed for increasing the size of nanoparticles from 2.4 to 4.0 nm. Monodispersity with relatively narrow size distribution ($\sigma/<d>$) of about 0.15, 0.18 and 0.22 and having the same elemental composition with the atomic percentage of $Fe_xPt_{100-x}$ ($x = 63$) are the main advantage of this method for particles with size of 3.2, 3.7 and 4.0 nm respectively.

**Acknowledgments** This work was supported by the Physics Research Center, Science & Research Branch at Islamic Azad University and the Magnetic & Superconducting Research Lab at Birjand University.

## References

1. D. Weller, A. Moser, L. Folks, M. E. Best, W. Lee, M. F. Toney, M. Schwickert, J. U. Thiele, and M. F. Doerner (2000). *IEEE Trans. Magn.* **36**, 10.
2. B. D. Cullity and C. D. Graham *Introduction to Magnetic Materials*, 2nd ed (John Wiley, New Jersey, 2009).
3. S. Sun, E. Fullerton, D. Weller, and C. B. Murray (2001). *IEEE Trans. Magn.* **37**, 1239.
4. V. S. Maceira, L. M. Lizmarzan, and M. Farle (2004). *Langmuir* **20**, 6946.
5. T. S. Vedantam and J. P. Liu (2003). *J. Appl. Phys.* **93**, 7184.
6. K. Yano, V. Nandwana, N. Poudyal, C. Rong, and J. Liu (2008). *J. Appl. Phys.* **104**, 013918.
7. S. Saita and S. Maenosono (2005). *Chem. Mater.* **17**, 3705.
8. S. Kang, S. Shi, G. X. Miao, Z. Jia, D. E. Nikles, and J. W. Harrell (2007). *J. Nanosci. Nanotechnol.* **7**, 350.
9. H. G. Bagaria, E. T. Ada, M. Shamsuzzoha, D. E. Nikles, and D. T. Johnson (2006). *Langmuir* **22**, 7732.
10. J. M. Vargas and R. D. Zysler (2007). *J. Appl. Phys.* **101**, 023903.
11. S. Sun, S. Anders, T. Thomson, J. E. E. Baglin, M. F. Toney, H. F. Hamann, C. B. Murray, and B. D. Terris (2003). *J. Phys. Chem. B.* **107**, 5419.
12. Y. C. Sui, Y. Zhao, M. Daniil, X. Z. Li, and D. J. Sellmyer (2006). *J. Appl. Phys.* **99**, 08G704.
13. L. C. Varanda and M. Jafelicci (2006). *J. Am. Chem. Soc.* **11062**, 128.
14. Y. Sasaki, M. Mizuno, A. C. C. Yu, T. Miyauchi, D. Hasegawa, T. Ogawa, M. Takahashi, B. Jeyadevan, K. Tohji, K. Sato, and S. Hisano (2005). *IEEE Trans. Magn.* **41**, 660.
15. C. Liu, X. Wu, T. Klemmer, N. Shukla, X. Yang, D. Weller, A. G. Roy, M. A. Tanase, and D. Laughlin (2004). *J. Phys. Chem. B.* **108**, 6121.
16. K. E. Elkins, T. S. Vedantam, J. P. Liu, H. Zeng, S. Sun, Y. Ding, and Z. L. Wang (2003). *Nano Lett.* **3**, 1647.
17. N. Poudyal, G. S. Chaubey, C. Rong, and J. P. Liu (2009). *J. Appl. Phys.* **105**, 014303.
18. K. Simeonidis, S. Mourdikoudis, I. Tsiaoussis, C. D. Samara, M. Angelakeris, and O. Kalogirou (2008). *J. Magn. Magn. Mater.* **320**, 2665.
19. S. Saita and S. Maenosono (2005). *Chem. Mater.* **17**, 6624.

20. O. Kalogirou, M. Angelakeris, C. D. Samara, S. Mourdikoudis, K. Simeonidis, K. Gloystein, A. V. Clemente, and I. Tsiaoussis (2010). *J. Nanosci. Nanotechnol.* **10**, 6017.
21. L. Colak and G. C. Hadjipanayis (2007). *J. Appl. Phys*. **101**, 09J108.
22. L. Colak and G. C. Hadjipanayis (2009). *Nanotechnology* **20**, 485602.
23. H. B. Wang, H. Wang, J. Zhang, F. J. Yang, Y. M. Xu, and Q. Li (2010). *Nanoscale Res Lett.* **5**, 489.
24. V. Nandwana, K. E. Elkins, N. Poudyal, G. S. Chaubey, K. Yano, and J. Ping Liu (2007). *J. Phys. Chem. C.* **111**, 4185.
25. S. Sun, H. Zeng, D. B. Robinson, S. Raoux, P. M. Rice, S. X. Wang, and G. Li (2004). *J. Am. Chem. Soc.* **126**, 273.
26. O. Masala and R. Seshadri (2005). *Chem. Phys. Lett.* **402**, 160.
27. Q. Song and Z. J. Zhang (2004). *J. Am. Chem. Soc.* **126**, 6164.
28. L. Zhang, R. He, and H. C. Gu (2006). *Mater. Res. Bull.* **41**, 260.
29. H. Reiss (1951). *J. Chem. Phys.* **19**, 482.
30. Y. Yin and A. P. Alivisatos (2005). *Nature* **437**, 664.
31. B. E. Warren *X-Ray Diffraction* (Dover Publications, New York, 1990).